Chapter 13

Spatio-Temporal Analysis of Sea Surface Temperature in the East China Sea Using TERRA/MODIS Products Data

Shaoqi Gong and Kapo Wong

Additional information is available at the end of the chapter

http://dx.doi.org/10.5772/intechopen.73217

Abstract

Sea surface temperature (SST) is an important parameter in determining the atmospheric and oceanic circulations, and satellite thermal infrared remote sensing can obtain the SST with very high spatio-temporal resolutions. The study first validated the accuracy of TERRA MODIS SST daytime and nighttime products with the timing SST measurements from the ships in the East China Sea (ECS) in February, May, August and November, 2001, and then the daily variation of daytime and nighttime SST difference was analyzed. Using 16-year MODIS SST monthly products data from February 2000 to January 2016, when all SST monthly products in February, May, August and November were averaged respectively, the seasonal spatial distribution pattern of SST in the ECS was discovered. After monthly sea surface temperature anomaly was finally processed by the empirical orthogonal function (EOF), the interannual variability of SST in the ECS was discussed. The results show that the MODIS SST daily products have a good accuracy with a mean absolute percentage error (MAPE) below 5%. The SST difference between day and night is the largest in winter, followed by spring, then for autumn and the smallest in summer, while the diurnal SST difference is very low for the same season in the different seas. The SST in the ECS displays the obvious seasonal spatial distribution pattern, in which the SST of winter is gradually increasing from north to south, while local temperature difference is the largest for 26.5°C in a year. In comparison, the SST in summer tends uniform and the difference is not more than 5°C in the whole sea. From the EOF analysis of SST anomaly, the interannual variability of SST in the ECS is affected by the East Asian monsoon, the latitudinal difference of solar radiation, the offshore circulation and the submarine terrain.

Keywords: spatio-temporal analysis, sea surface temperature, East China Sea, MODIS SST product, empirical orthogonal function

1. Introduction

Sea surface temperature (SST) can display the comprehensive results of solar radiation, ocean-atmosphere interactions and oceanic inner dynamic and thermal processes. It is not only an important physical parameter for studying the exchange of water vapor and heat between sea surface and atmosphere but also provides an useful index for oceanographic studies such as ocean circulation, water mass, ocean front, upwelling current, seawater mixing [1] and ocean ecological environment [2]. Since SST anomalies of 0.5–2.0 K in the Pacific Ocean during El Nino or La Nina is sufficient to cause abnormality in oceanic and atmospheric circulations and global weather patterns, the global ocean surface temperature should be observed continuously [3]. With the development of satellite thermal infrared remote sensing for recent more than 30 years, the SST retrieved from thermal infrared images with the very high spatio-temporal resolutions, large-scale and periodic characteristics will be useful data sources for oceanography. At present, the NOAA/AVHRR Pathfinder SST product was applied widely in some researches about SST in the local sea [4–7]. Since the low spatial resolution with 0.25° × 0.25°, AVHRR Pathfinder SST product is inconvenient to the research for local sea. The sensor MODIS onboard TERRA and AQUA satellite in the Earth Observation System can revisit four times per day, which provides the SST with the high spatio-temporal resolutions for the oceanographic research [8, 9]. In view of the advantage and less reports on the MODIS SST products, this chapter will use the MODIS SST products data to analyze the spatio-temporal variation of SST in the East China Sea (ECS). It is helpful to discover the SST change mechanisms and its influence factors in the ECS, discuss the relationship between China offshore and ENSO and understand the effect of China offshore on continental climate.

2. Data and methods

2.1. Research area

The East China Sea (ECS) is located in the east of China's continent and is a broad continental shelf bounding the North Pacific Ocean in the west, which covers an area of about 1.22×10^6 km^2 and includes Bohai Sea, Huanghai Sea and Donghai Sea within the Korean Peninsula, Kyushu, Ryukyu Islands and Taiwan island. The submarine terrain is very complex in the ECS, the depth contour is paralleled with the coastline and the topography is leaned from northwest toward southeast and is the steepest in the southeastern continental margin. Bohai Sea approximates an inland sea with a mean depth of 18 m and the largest depth of 85 m, while Huanghai Sea is a semi-enclosed sea with a mean depth of 40 m, which has a largest depth of 140 m in the north of Jeju Island. Donghai Sea is a marginal sea where the mean depth of continental shelf is 72 m, of which whole sea is 349 m and the largest depth is 2700 m in the west of Okinawa Island. The ECS undergoes temperate and subtropical climate, where the northerly wind prevails in winter and the southerly wind does in summer. Influenced by the solar radiation, sea surface temperature is gradually increasing from north to south. The ocean circulation in the ECS is determined jointly by the offshore circulation and coastal currents. The offshore circulation includes Kuroshio Current, Taiwan Warm Current, Tsushima Current and Huanghai Warm

http://dx.doi.org/10.5772/intechopen.73217

Current, while the coastal currents are produced by the runoff with low salinity from rivers and the wind currents affected by the East Asian monsoon. However, these ocean circulations will result in the spatial and temporal variations of sea surface temperature and salinity in the ECS.

2.2. Sea surface temperature

Since satellite TERRA respectively passes once by the ECS in the day and night, NASA/GSFC develops the MODIS SST daytime and nighttime daily products, and monthly products are

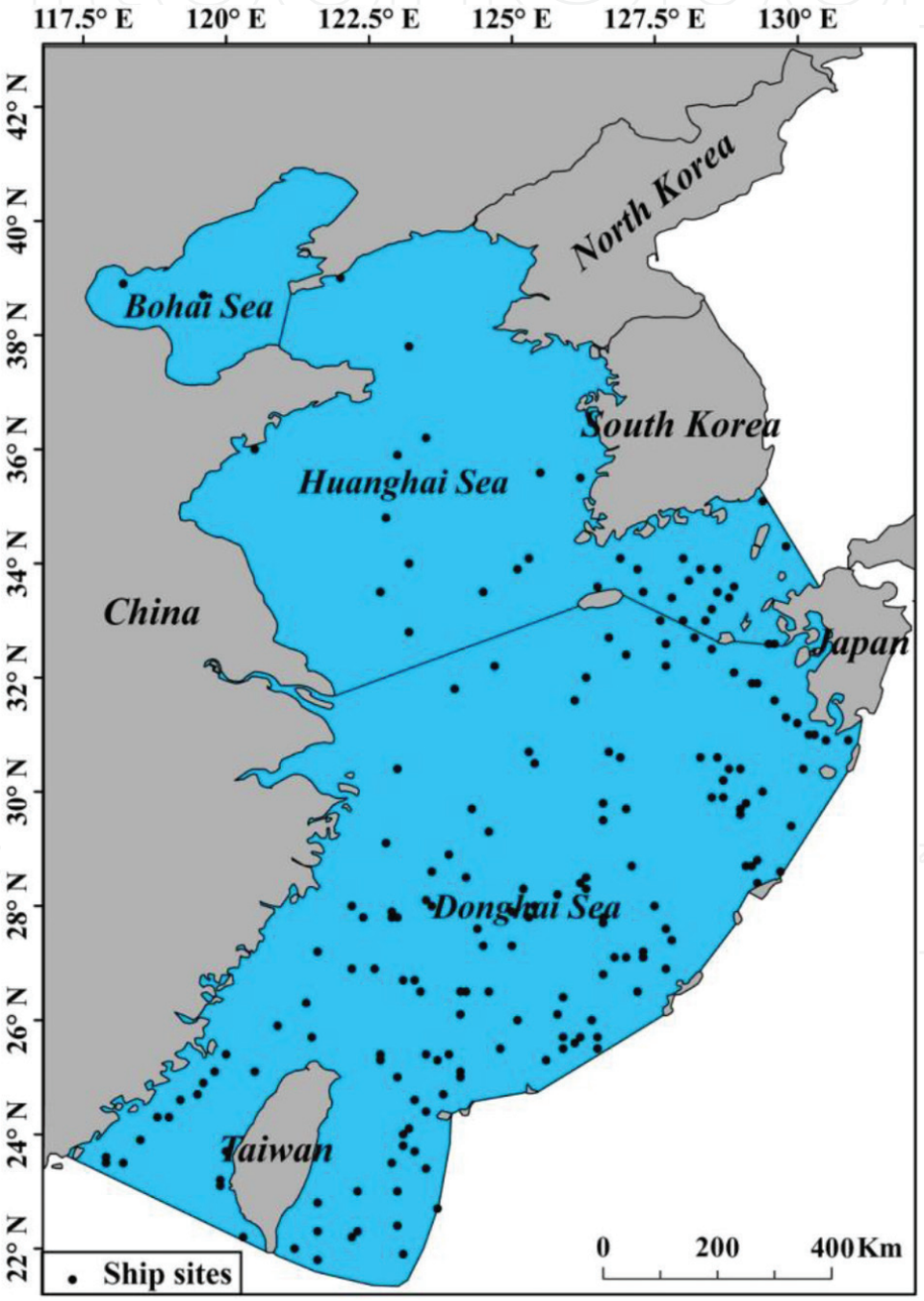

Figure 1. Distribution of ship locations and East China Sea.

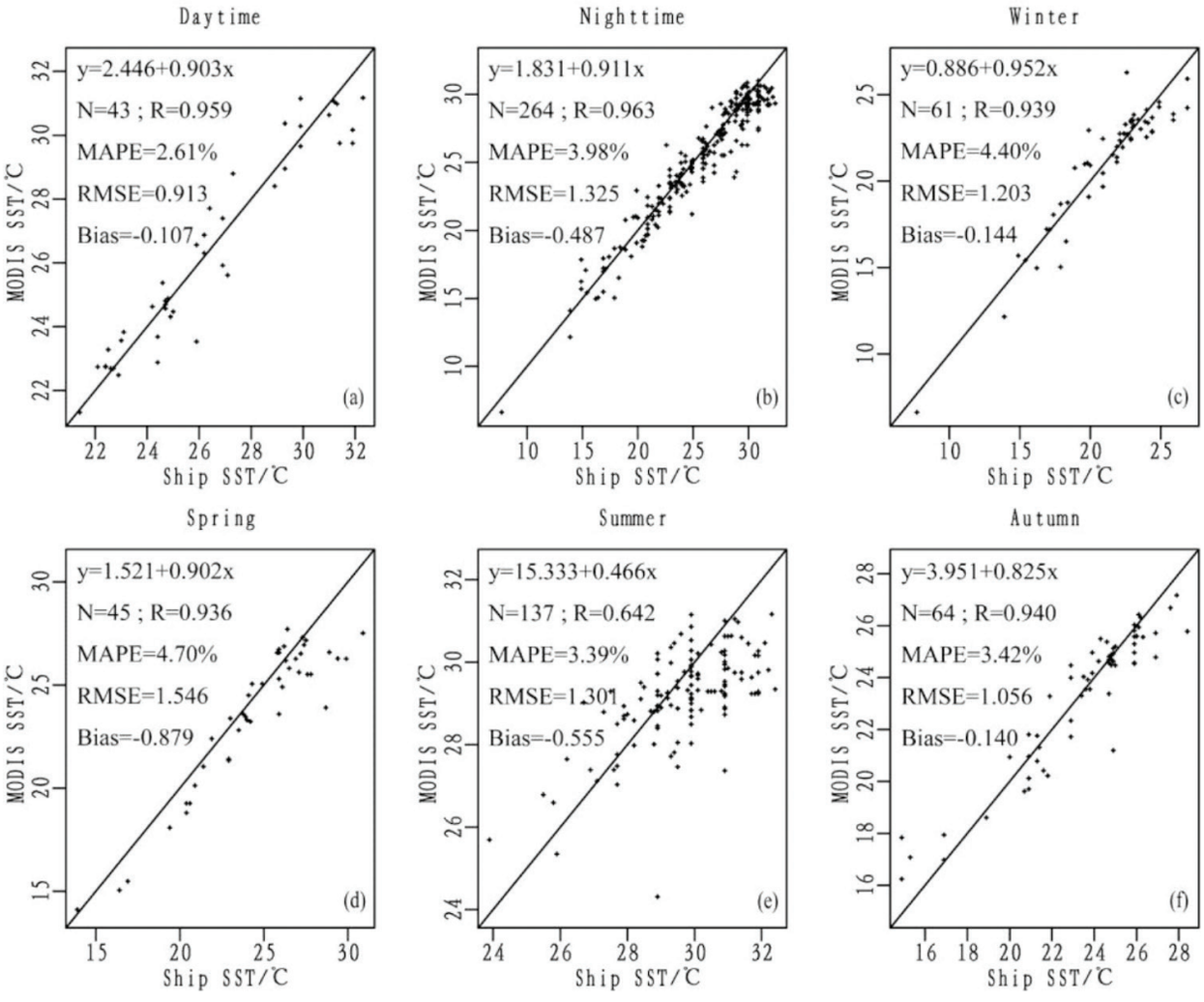

Figure 2. SST scatter plots between MODIS daily products and ship measurements.

aggregated by the mean of daily products in 1 month. In order to use MODIS SST monthly products in the study, MODIS SST daytime and nighttime products are validated with the timing SST measurements from the ships in the ECS in February, May, August and November of 2001, which represent for the winter, spring, summer and autumn. Due to 1-hour ship-measuring interval of SST, MODIS SST daily products can match well with those of ship measurements. And the distribution of ship locations can be seen from **Figure 1**. The ship SST measurements are available from the China Meteorological Data Network (http://data.cma.cn/). The 16-year MODIS SST monthly products from February 2000 to January 2016 are used to analyze the temporal variation of SST in the ECS. All the MODIS SST products data with the spatial resolution of 4 km were downloaded from the global ocean color network (https://oceancolor.gsfc.nasa.gov/).

2.3. Data processing method

In order to validate the accuracy of MODIS SST daily products, ship SST measurements were screened by comparing with the passing time of satellite TERRA, and time difference of both data is limited within 1 hour. The measuring locations of ships according to their geographical

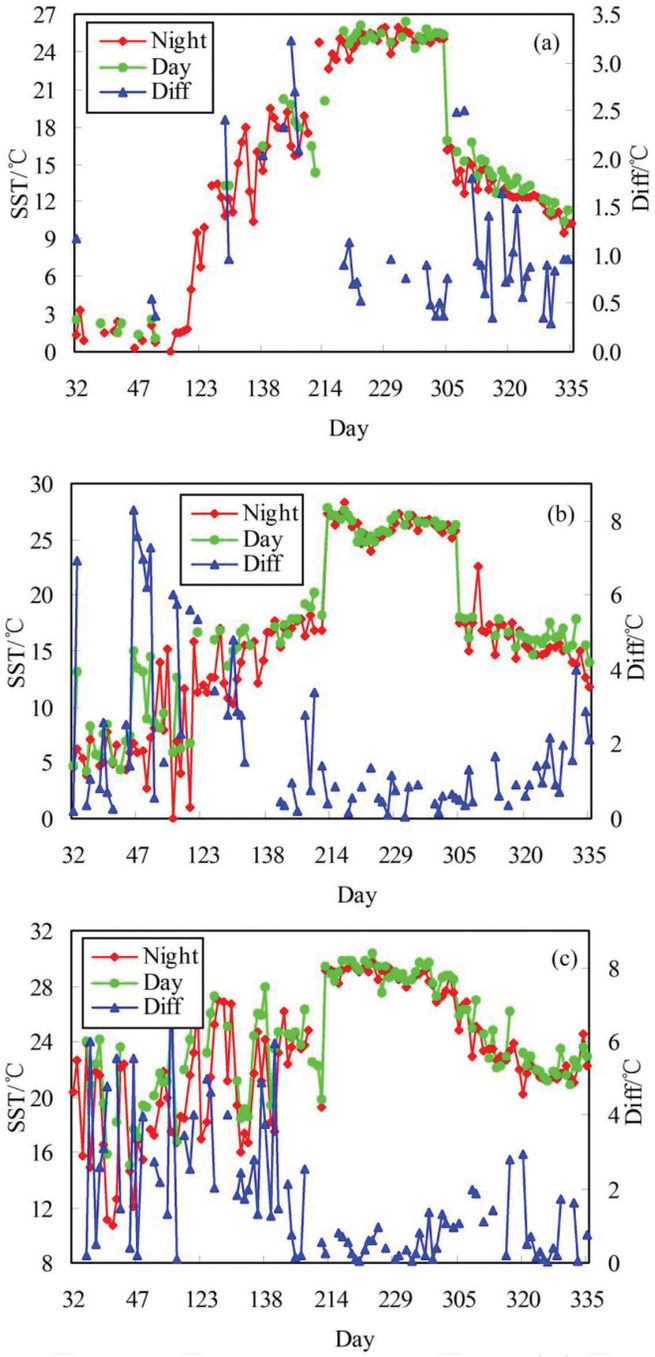

Figure 3. SST variation charts for every day and night in the East China Sea ((a–c) stands for Bohai Sea, Huanghai Sea and Donghai Sea).

	Bohai Sea	Huanghai Sea	Donghai Sea
Winter		3.569	2.887
Spring	2.248	2.262	2.526
Summer	0.696	0.598	0.518
Autumn	1.043	1.332	1.001

Table 1. Average diurnal temperature difference for the different seasons in three seas.

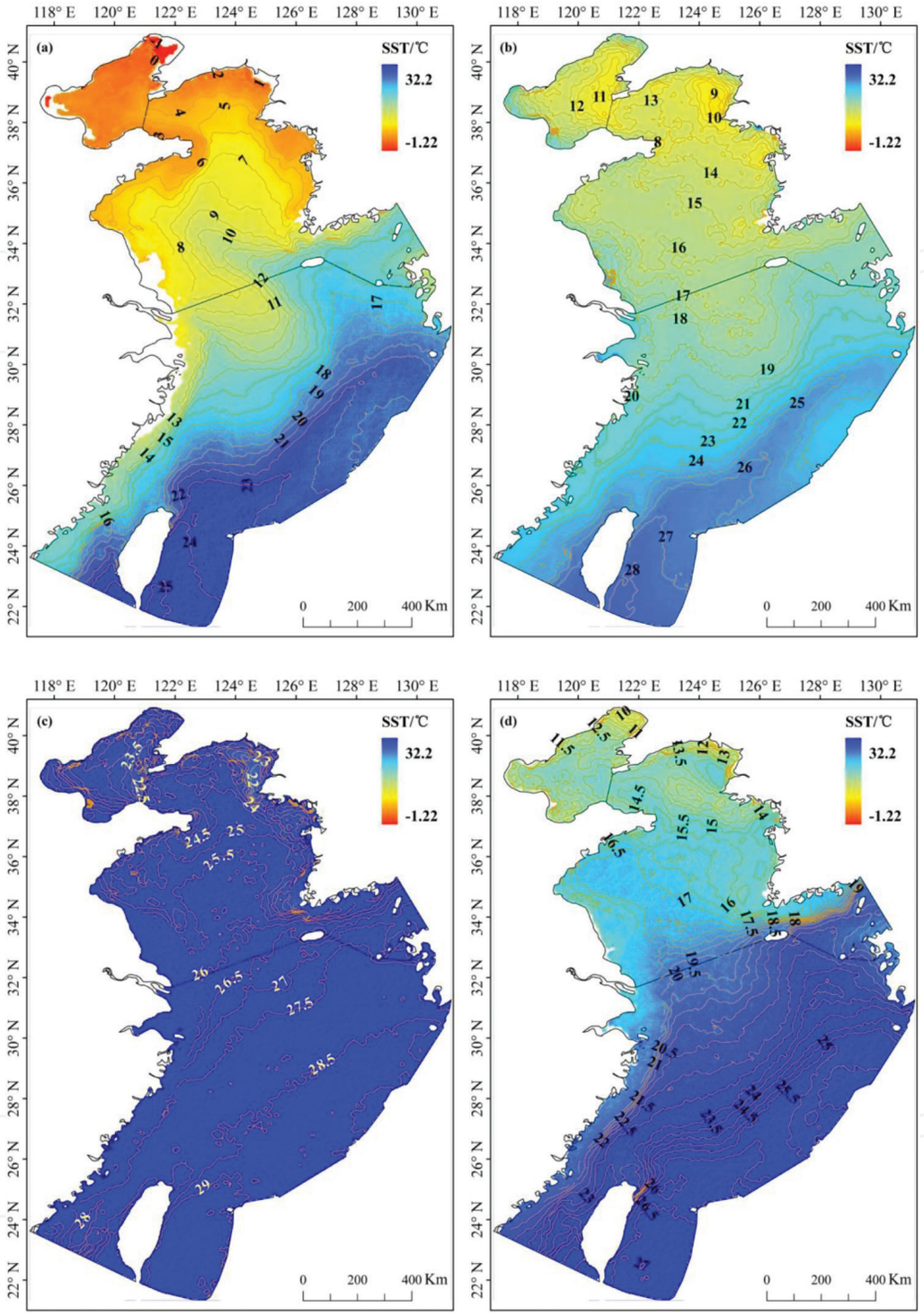

Figure 4. SST seasonal distribution maps in the East China Sea: (a) winter; (b) spring; (c) summer and (d) autumn.

Eigenvector	1	2	3	4	5	6
Percent	21.22	7.24	4.57	3.07	2.80	1.99
Cumulative percent	21.22	28.46	33.03	36.10	38.90	40.89

Table 2. Contributions of the first six eigenvectors to variance.

http://dx.doi.org/10.5772/intechopen.73217

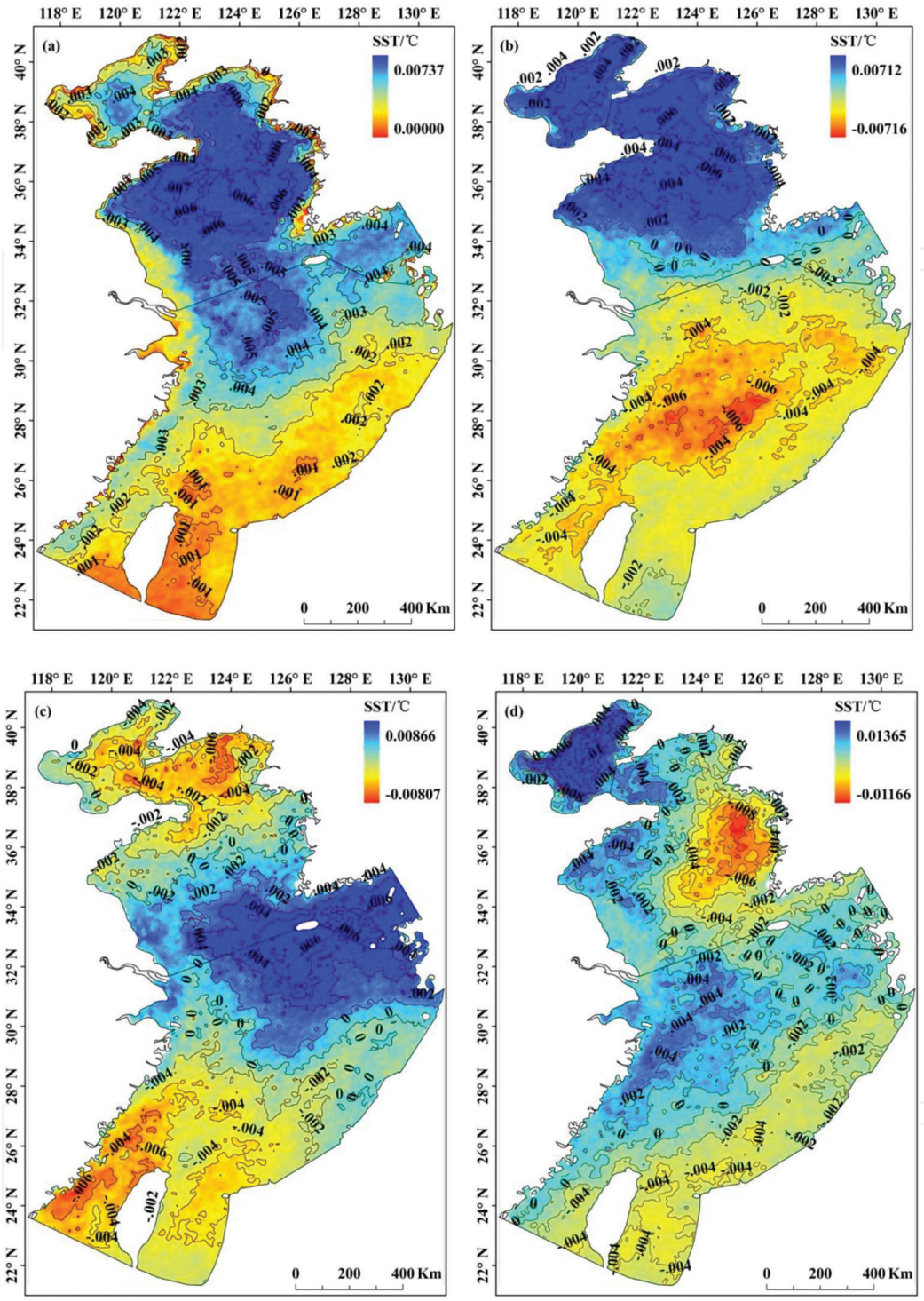

Figure 5. Spatial distribution maps of first four SST eigenvectors in the ECS: a-d for the SST eigenvector from first to fourth, respectively.

coordinates are corresponding to the images of MODIS SST daily products, and the median of the 3 × 3 neighborhood pixels around the central location is calculated in the SST images. The SST scatter plots between MODIS and ships are drawn for the different seasons, day and night, respectively (**Figure 2**), and the relative errors are calculated for MODIS SST daily products.

To analyze the SST difference between day and night in the ECS, the vector boundary maps of Bohai Sea, Huanghai Sea and Donghai Sea were overlapped on the images of MODIS SST daytime and nighttime products, and the mean of all the pixels within the zone of each sea is calculated after the outliers were removed. The calculated SST values of three seas in the daytime and nighttime in 2001 are used to draw the daily SST variation chart (**Figure 3**). The average diurnal SST difference is calculated for the three seas in the different seasons (**Table 1**).

The mean of MODIS SST daytime monthly products for February, May, August and November from February 2000 to January 2016 was calculated after the outliers were excluded in the SST images. The average SST images of the four months stand for winter, spring, summer and autumn were used to analyze the seasonal variations of SST in the ECS. When the average SST images of the four months are clipped by the vector map of ECS, the SST seasonal distribution maps in the ECS are shown in **Figure 4**.

In order to analyze the interannual variability of SST in the ECS, all the MODIS SST daytime monthly products were firstly carried out the climatological mean, that is, all the SST monthly products from January to December were averaged after the outliers were removed in the SST images. Secondly, the each monthly product was subtracted to the corresponding monthly mean SST so that the seasonal and inner-annual cyclicity of SST is eliminated, then the monthly sea surface temperature anomaly was obtained [10, 11]. Finally, 192 SST anomaly

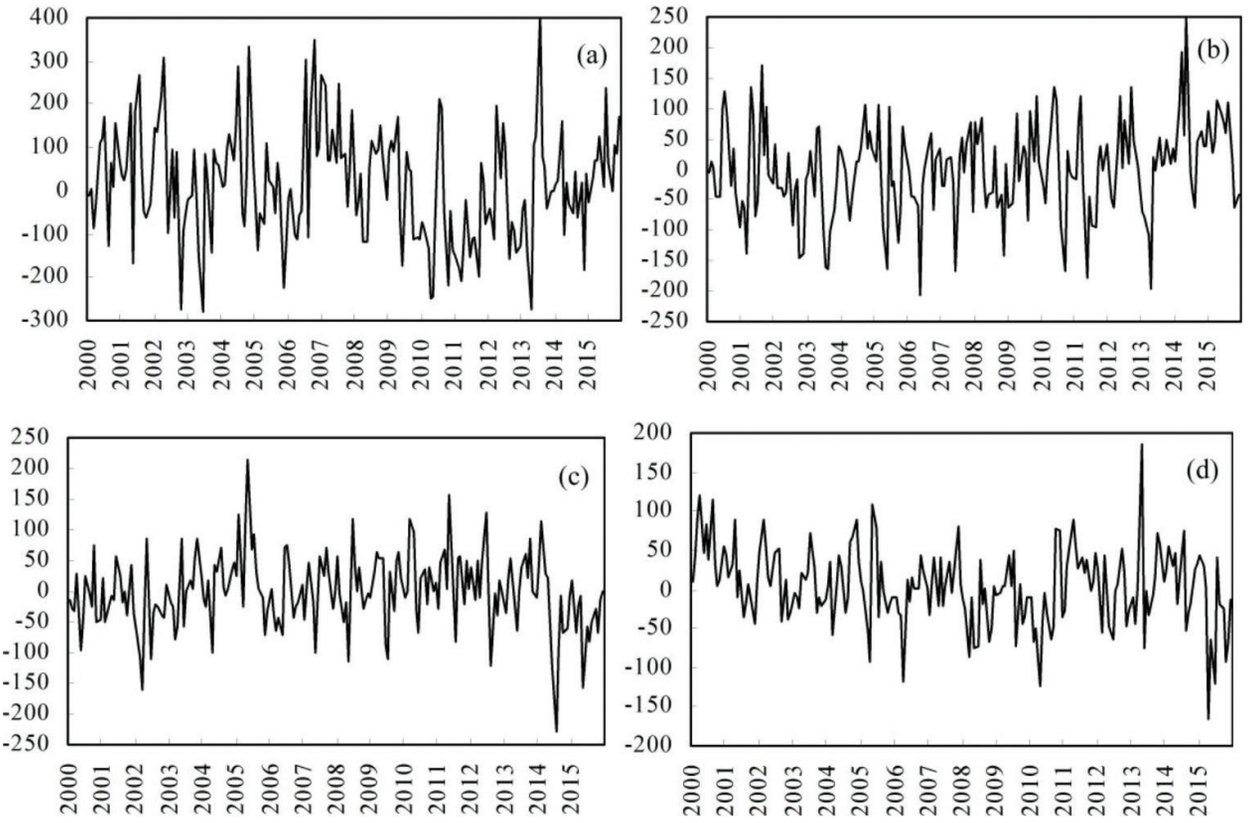

Figure 6. Time coefficient charts of first four SST eigenvectors in the ECS. (a-d) stands for the time coefficient of SST eigenvector from first to fourth, respectively.

http://dx.doi.org/10.5772/intechopen.73217

images were carried out the empirical orthogonal function analysis, and the eigenvalues and eigenvectors of SST were calculated in the ECS [12–14]. **Table 2** shows the contributions of the first six eigenvectors to SST variance, and then the first four SST eigenvectors map in the ECS and their corresponding time coefficient charts are shown in **Figures 5** and **6**, respectively.

3. Results and discussion

3.1. Accuracy evaluation of MODIS SST daily products

Since the MODIS SST global daytime and nighttime products were generated by MODIS raw images which were obtained by simultaneous satellite TERRA passes through the earth and undergo the preprocess, retrieval and mosaicking. Then, the monthly products were aggregated by the mean of daily products in a month. Utilizing MODIS SST monthly products to analyze the SST spatio-temporal variation in the ECS, the accuracy of MODIS SST daily products should be evaluated first. MODIS SST daytime and nighttime products in February, May, August and November, 2001, which represent for the winter, spring, summer and autumn, selected to compare with the ship SST measurements, and the time difference of both SST is not more than 1 hour. **Figure 2** shows the SST scatter plots between MODIS and ship for the different seasons, day and night, respectively. It can be seen from **Figure 2** that all the matched SST points are located near the scatter plot 1:1 line. The slopes of majority scatter plots are above 0.902 except for summer of 0.466 and autumn of 0.825, and the correlation coefficients of majority scatter plots are more than 0.936 besides summer of 0.642, which indicate that MODIS SST daily products are in a very good agreement with the ship SST measurements. The biases in all the scatter plots are below 0, indicating that MODIS SST daily products are little lower than that of ships. Gentemann [15] compared the AUQA/MODIS sea surface temperature with in situ SST measurements made by drifting and moored buoys, and the bias of MODIS SST was found to be −0.13°C. This result is similar to the bias of daytime, winter and autumn in the study. Qiu et al. [16] validated AVHRR SST with drifting buoy SST in the northern South China Sea and showed the biases of AVHRR SST are −0.43 and −0.33°C for daytime and nighttime, respectively. These biases are also closed to that of MODIS SST in this study, which are −0.107 and −0.487°C for daytime and nighttime, respectively. The mean absolute percentage errors (MAPE) in all the scatter plots are below 5%, indicating MODIS SST daily products have a low uncertainty, high precision and good quality. The number of MODIS matched SST points in the daytime is 43, and the bias, root mean square error (RMSE) and MAPE are −0.107, 0.913°C and 2.61%, respectively (**Figure 2(a)**), which are lower than those in the nighttime that are −0.487, 1.325°C and 3.98%, respectively (**Figure 2(b)**). This figure shows that the accuracy of MODSI SST daytime product is superior to the nighttime one. Comparing three error indices of MODIS SST daily products in the different seasons (**Figure 2(c–f)**), the errors in autumn are the smallest, the second for winter except for MAPE of 4.40%, then for summer and the errors in spring are the biggest. Hence, the accuracy of MODIS SST daily products indicates seasonal variation in descending order from autumn to winter, to summer and then to spring. On the whole, MODIS SST daily products have a good accuracy with the MAPE below 5%.

3.2. Variation of the diurnal SST difference in the ECS

Utilizing MODIS SST daytime and nighttime products in February, May, August and November 2001, the average SST within Bohai Sea, Huanghai Sea and Donghai Sea was calculated every day after the outliers were excluded in the SST product images. **Figure 3** shows the SST variation charts for daytime, nighttime and diurnal difference in the three seas, and x-axis stands for the day of year, 32–59 for February, 121–151 for May, 213–243 for August and 306–335 for November. From **Figure 3**, it is clear that the daytime SST is higher than nighttime one and the diurnal SST difference is positive. Except that the matched number of daytime and nighttime SST is a few in Bohai Sea in winter, the diurnal SST difference in the other two seas is the largest in winter, and that in spring is the second for three seas, while the difference in autumn is very small, and the smallest for summer. **Table 1** shows the average diurnal SST differences for the three seas in the different seasons. The average diurnal difference is 3.569 and 2.887°C for Huanghai Sea and Donghai Sea, respectively, in winter, and that is 2.248, 2.262 and 2.526°C in the Bohai Sea, Huanghai Sea and Donghai Sea, respectively, in spring, then 1.043, 1.332 and 1.001°C for the three seas in autumn, while in summer for the three seas is 0.696, 0.598 and 0.518°C, respectively. Thus, the diurnal SST difference is very distinguishing, while that becomes little in the different seas for the same season. The variation of diurnal SST difference could have a good relationship with the length of daytime and nighttime in the different seasons. The daytime is short and nighttime is long in the north hemisphere in winter, and the solar radiation is absorbed less by the sea surface in the daytime due to short sunshine duration, while the more energy is emitted from the sea surface in the nighttime, which results in the large diurnal SST difference in winter, and the vice versa for summer. Since spring and autumn are the transitional season between winter and summer, the variation of diurnal SST difference in spring and autumn is moderate.

3.3. Seasonal spatial pattern of SST in the ECS

Figure 4 shows the SST seasonal spatial distribution maps drawn by the average MODIS SST monthly products for February, May, August and November from February 2000 to January 2016, and **Figure 4a–d** stands for winter, spring, autumn and summer. Since the East China Sea is located in the East Asian monsoon zone, the SST displays the typical seasonal variability.

Figure 4(a) shows the SST spatial distribution map in winter, in which the SST is gradually increasing from north to south in winter and local temperature difference is the largest for 26.5°C in a year. This is due to the much change of solar radiation with the latitude in winter. In the Bohai Sea, the variation of SST is generally not large, and the average temperature is 1.6°C in the whole sea. The minimum temperature is about −1.22°C in the top of Liaodong Bay, while the maximum one is 3.9°C in the Bohai strait. The obvious variation of SST is seen the north-south and east-west direction in the Bohai Sea, which the SST is increasing to 3.0°C from Liaodong Bay to Laizhou Bay for the north-south direction and is decreasing to −0.8°C from Bohai strait to Bohai Bay for the east-west direction. This SST distribution pattern displays the characteristic of low temperature in the shallows and high one in the profundal zone. The average SST is 6.9°C in the Huanghai Sea, and the low temperature zone is located in the eastern and western coastal waters, while the high temperature area is in the southeast

http://dx.doi.org/10.5772/intechopen.73217

and middle of the Sea. The minimum temperature is about 1.5°C in the West Korea Bay, then for the coasts of Korean Peninsula and Shandong Peninsula about 3.0°C. The possible factors for the low SST in these areas are the influence of the continental air temperature and the coastal currents [1, 17]. The maximum temperature can reach at 15.8°C in the Korea Strait, then in the middle of Huanghai Sea about 14.0°C, which is affected by the Huanghai Warm Current and results from the extend of currents with high temperature and salinity from the east of Jeju Island to west by north. The average SST is 17.6°C in the Donghai Sea, and the low temperature zone is below 11°C and situated in the northwest of the Sea and the western coastal waters included the narrow area near the coast from the mouth of the Yangtze River to Taiwan strait, which is mainly affected by the coastal currents in the Donghai Sea shelf. However, the temperature in the open waters is very high between 16.0 and 25.5°C which is influenced jointly by the Kuroshio current and Taiwan warn current [6, 18].

Since spring is the transitional season from winter to summer, the SST spatial distribution pattern in spring is very different from that of winter. As seen from **Figure 4(b)**, the SST in the Bohai Sea is contrary to the winter, which the temperature is high in the coastal shallows and low in the profundal zone. The average SST is 14.2°C in the Bohai Sea in spring, and the maximum temperature is close to 20.0°C in Liaodong Bay, Bohai Bay and Laizhou Bay while the minimum one is about 10.0°C in the north of Bohai strait. The SST in the Bohai Sea is first controlled by the terrain and solar radiation and second by the circulation [17]. The average SST is 14.9°C in the Huanghai Sea, and the temperature is much lower in the northeast of the Sea, especially in the West Korea Bay, then for the southern coastal waters of Korean Peninsula where the minimum temperature is about 9.0°C. The temperature is very high in the southwestern coastal waters and the Korea Strait where it is close to 19.0°C. The average SST is 22.4°C in the Donghai Sea, and the SST in the middle-north of the Sea is relatively low for 17°C or so, then the medium is in the eastern and western coastal waters for 20.8°C, while the temperature is very high in the southeastern open waters and it is above 25°C, especially in the waters around Taiwan reaching to 28°C.

Due to the strong solar radiation in summer, the SST in the ECS trends uniform and the temperature difference in the northern-southern sea area is not more than 5°C (**Figure 4(c)**). The average SST in the Bohai Sea is 24.7°C, the maximum temperature reaches to 27°C in the Laizhou Bay, while the minimum one is about 23.5°C in the west of Bohai Strait and the middle of Bohai Sea. The cold waters are caused by the upwelling current from the deep seawater. In the Huanghai Sea, the SST is relatively lower between 23 and 24.5°C in the eastern coastal waters that are located in the West Korea Bay and west of Korean Peninsula. Then, the SST is also low about 24°C in the western coastal waters of Shandong Peninsula and the north of Jiangsu. The low SST zone is formed by the gradient submarine terrain and the strong tides together [10, 18]. The SST in middle of the Huanghai Sea is very uniform and high for 25°C or so, hence the summer average temperature is 25.2°C in the Huanghai Sea. The SST difference is very little in the Donghai Sea with the mean for 28°C. The low temperature waters are still situated in the western coasts, which are the coasts of Zhejiang and Fujian provinces with the minimum temperature at 25.5°C. The low temperature zone is mainly formed by the coastal upwelling current. However, the overall SST is very high in the open waters of Donghai Sea with the peak at 29°C.

Autumn is also the transitional season from summer to winter, and the SST in this season drops most quickly and becomes gradually lower from south to north in the ECS (**Figure 4(d)**). In the Bohai Sea, the SST in the shallows near the coast turns low about 10°C, such as Liaodong Bay, Bohai Bay and Laizhou Bay, while that in the middle of the sea is relatively high about 13.5°C, so the average SST within the whole Bohai Sea is 13.0°C in autumn. In the Huanghai Sea, the SST is relatively low in the eastern and western coastal waters, especially in the West Korea Bay with the temperature between 12 and 13.5°C. There is a warm water zone from south to west, even reaching to the Qingdao coast where the SST is within 16.5–20.0°C. This is probably caused by the Huanghai coastal current, which is evolved from the convergence of southward Huanghai Warm Current and inland freshwater from the Shandong Peninsula [18]. And the average SST of whole Huanghai is 16.2°C in autumn. In the Donghai Sea, the SST gets gradually low from south to north and the largest temperature difference approaches to 7°C, then the average SST is 23.3°C within the whole sea. The western coastal waters are still the low temperature zone where the SST is within 15.0–20.5°C, and the SST in the west of Kyushu Island is also very low about 22°C. There is a low temperature water area in the north of Taiwan Island at 23°C, which has something with the anticyclonic mesoscale eddy in autumn. However, the relatively high SST is in the east of Taiwan Island with the maximum one of 27°C.

3.4. The EOF analysis of the SST interannual variability in the ECS

Figure 5 shows the spatial distribution maps of first four SST eigenvectors in the ECS, and their contributions to the SST variance are 21.22%, 7.24%, 4.57% and 3.07% (**Table 2**). The SST variability of first eigenvector is completely positive in the ECS, and this shows that the SST variation tendency appears a good consistence in the whole Sea and indicates further the influence of East Asian monsoon climate on the SST interannual variability of ECS [19]. The SST variability is relatively high above 0.006°C in the Huanghai Sea, then for the north of Donghai Sea, which is caused by the Huanghai Warm Current in winter and the cold water mass in summer [17]. **Figure 6(a)** shows the time coefficient chart of first SST eigenvector; when the time coefficient is positive, the SST within the whole Sea is increasing. And the SST falls for the negative time coefficient. The SST variability of second eigenvector displays the opposite distribution pattern in the north and south, and it is positive in the Bohai Sea and Huanghai Sea and is negative in the Donghai Sea (**Figure 5(b)**), which indicates the influence of latitude and solar radiation on the SST interannual variability [20, 21]. The latitude is relatively high in the Bohai Sea and Huanghai Sea, where the seasonal difference of solar radiation is very large, so the SST interannual variability is a little higher there, but the contrary for the Donghai Sea. In the time coefficient chart of second SST eigenvector (**Figure 6(b)**), when the time coefficient is positive, the SST in the Bohai Sea and Huanghai Sea will rise and that in the Donghai Sea will drop. While the time coefficient is negative, the SST in the northern and southern Sea will occur the opposite variation. The SST variability of third eigenvector reflects the influence of ocean current (**Figure 5(c)**) [18, 21], the variability is mainly negative and the negative central area is located in the middle of Bohai Sea, the north of Huanghai Sea and the west of Taiwan Island where are affected by the Huanghai Warm Current and coastal current. The sea area with negative variability is very small, which mainly distributes in the around Jeju Island included the southeast of Huanghai Sea and the east of Donghai Sea, and they are often controlled by the Tsushima Current. As seen from **Figure 6(c)**, most of the time coefficients are negative. This

http://dx.doi.org/10.5772/intechopen.73217

shows that the SST of the majority of sea areas rises except that around the Jeju Island falls. The SST variability of fourth eigenvector indicates the effect of submarine terrain on the SST interannual variability of ECS (**Figure 5(d)**). The central area of positive variability is situated in the Bohai Sea, the western coast of Huanghai Sea and the northwest of Donghai Sea where the variability is above 0.004°C, while that of negative variability is below −0.008°C in the west of Korean Peninsula. These areas are near the coasts with lower water depth and are the SST influenced easily by the coastal currents and the continental atmospheric temperature. Hence, the SST variability is very small in the middle of Huanghai Sea and the south of Donghai Sea due to the greater water depth. **Figure 6(d)** shows more positive time coefficients and less negative ones in the chart of fourth SST eigenvector, which means that the SST of the wide range sea area is increasing and that of only small-scale area is decreasing. Furthermore, the maximum positive time coefficient and minimum negative one are smaller than other eigenvectors, indicating that the SST variability becomes more insignificant for the fourth eigenvector.

4. Conclusions

Based on the validation of MODIS SST daytime and nighttime products using the ship SST measurements in the East China Sea (ECS), this chapter discusses the variation of diurnal SST difference for the three seas in the different seasons and analyzes the SST seasonal and interannual variability in the ECS. Conclusions can be summarized as:

1. Comparison with the ship SST measurements, the MODIS SST daily products have a good accuracy with a mean absolute percentage error below 5%. The accuracy of MODSI SST daytime products is superior to the nighttime ones. The accuracy of MODIS SST daily products indicates the seasonal variation in descending order from autumn to winter, to summer and then to spring.
2. Analyzing the SST of daytime and nighttime for the three seas in the ECS, the diurnal SST difference is the largest in winter, followed by spring, then for autumn, and the smallest in summer, while the difference is very little for the same season in the different seas. The variation of diurnal SST difference could have a good relationship with the length of daytime and nighttime in the different seasons.
3. The SST in the ECS displays the obvious seasonal spatial distribution pattern, in which the SST in winter is gradually increasing from north to south and local temperature difference is the largest for 26.5°C in a year, while the SST in summer tends uniform due to the strong solar radiation and the difference is not more than 5°C in the whole sea. Since spring and autumn are the transitional seasons between winter and summer, the SST changes quickly in spring and autumn. The SST seasonal spatial variability in the ECS is mainly attributed to the solar radiation, continental atmospheric temperature, coastal currents and offshore circulation, such as Huanghai Warm Current, Tsushima Warm Current, Kuroshio Current and Taiwan Warm Current.
4. From the EOF analysis of SST anomaly, the interannual variability of SST in the ECS is affected by the East Asian monsoon, the latitudinal difference of solar radiation, the offshore circulation and the submarine terrain.

Acknowledgements

This work was funded by the National Research and Development Program of China (NO. 2016YFC1402003). The authors thank the China Meteorological Data Network (http://data.cma.cn/) and the global ocean color network (https://oceancolor.Gsfc.nasa.gov/) for providing the ship SST measurements and TERRA/MODIS SST products, respectively. The authors also appreciate the help from Dr. Xue Li in Xiamen University, China for the SST EOF analysis.

Author details

Shaoqi Gong[1]* and Kapo Wong[2]

*Address all correspondence to: shaoqigong@163.com

1 School of Geography and Remote Sensing, Nanjing University of Information Science and Technology, Nanjing, China

2 Chinese University of Hong Kong, Center for Housing Innovations, Shatin, Hong Kong

References

[1] Bao X, Wan X, Gao G, Wu D. The characteristics of the seasonal variability of the sea surface temperature field in the Bohai Sea, the Huanghai Sea and the East China Sea from AVHRR data. Acta Oceanologica Sinica. 2002;**24**(5):125-133

[2] Ji C, Zhang Y, Tsou JY. Evaluating the impact of sea surface temperature (SST) on spatial distribution of chlorophyll-a concentration in the East China Sea. International Journal of Applied Earth Observation and Geoinformation, 2018. Accepted

[3] Chan P, Gao B. A comparison of MODIS, NCEP, and TMI sea surface temperature datasets. IEEE Geoscience and Remote Sensing Letters. 2005;**2**(3):270-274

[4] Keiner LE, Yan X. Empirical orthogonal function analysis of sea surface temperature patterns in Delaware Bay. IEEE Transactions on Geoscience and Remote Sensing. 1997; **35**(5):1299-1306

[5] Ryan H, Igor B, Peter C, Zhengqiang S. Climatology and seasonal variability of ocean fronts in the East China, Yellow and Bohai Seas from satellite SST data. Geophysical Research Letters, 2000;**27**(18):2945-2948

[6] Chente T, Chiyuan L, Shihchin C, Chungzen S. Temporal and spatial variations of sea surface temperature in the East China Sea. Continental Shelf Research. 2000;**20**:373-387

[7] Lee M, Yeah C, Cheng C, Chan J, Lee K. Empirical orthogonal function analysis of AVHRR sea surface temperature patterns in taiwan strait. Journal of Marine Science and Technology. 2003;**11**(1):1-7

[8] Kilpatrick KA, Podestá G, Walsh S, Williams E, Halliwell V, Szczodrak M, Brown OB, Minnett PJ, Evans RA. decade of sea surface temperature from MODIS. Remote Sensing of Environment. 2015;**165**:27-41

[9] Hosoda K, Murakami H, Sakaida F, Kawamura H. Algorithm and validation of sea surface temperature observation using MODIS sensors aboard Terra and Aqua in the western north Pacific. Journal of Oceanography. 2007;**63**:267-280

[10] Won-Sun P, Im Sang O. Interannual and interdecadal variations of sea surface temperature in the East Asian Marginal Seas. Progress in Oceanography. 2000;**47**:191-204

[11] Fang G, Chen H, Wei Z, Wang Y, Wang X, Li C. Trends and interannual variability of the South China Sea surface winds, surface height, and surface temperature in the recent decade. Journal of Geophysical Research. 2006;**111**:C11S16. DOI: 10.1029/2005JC003276

[12] Smith TM, Reynolds RW, Livezey RE, Stokes DC. Reconstruction of historical sea surface temperatures using empirical orthogonal functions. Journal of Climate. 1996;**9**:1403-1420

[13] Borzelli G, Ligi R. Empirical orthogonal function analysis of sst image series: A physical interpretation. Journal of Atmospheric and Oceanic Technology. 1999;**16**:682-690

[14] Alvarez A, Lopez C, Riera M, Hernandez-Garcia E, Tintore J. Forecasting the SST space-time variability of the Alboran Sea with genetic algorithms. Geophysical Research Letters. 2000;**27**(17):2709-2712

[15] Gentemann CL. Three way validation of MODIS and AMSR-E sea surface temperatures. Journal Geophysical Research, Oceans. 2014;**119**:2583-2598. DOI: 10.1002/2013JC009716

[16] Qiu C, Wang D, Kawamura H, Guan L, Qin H. Validation of AVHRR and TMI-derived sea surface temperature in the northern South China Sea. Continental Shelf Research. 2009;**29**:2358-2365

[17] Zeng G, Lian S, Cheng X, Hua Z, Qi YEOF. Analysis of intra-seasonal variabilities of SST in the East China Sea and Yellow Sea. Advances in Marine Science. 2006;**24**(2):146-155

[18] Zhao Q, Tian J, Cao C, Wang Q. The numerical simulation and the assimilation technique of the current and the temperature field in the Bohai Sea, Huanghai Sea and East China Sea. Acta Oceanologica Sinica. 2005;**27**(1):1-6

[19] Wu Y, Cheng G, Han G, Shu Y, Wang D. Analysis of seasonal and intcrannual variability of Sea surface temperature for China Seas based on CORA dataset. Acta Occanologica Sinica. 2013;**35**(1):44-54

[20] Zhang J, Liu Q, Wu S. The analysis of interannual and interdecadal characteristics of global sea surface temperature. Acta Oceanologica Sinica. 2010;**32**(4):24-31

[21] Zhang S, Yu F, Diao X, Guo J. The characteristic analysis on sea surface temperature inter-annual variation in the Bohai Sea, Yellow Sea and East China Sea. Marine Science. 2009;**33**(8):76-91

IntechOpen